Journal of Arid Environments 73 (2009) 844–853

Contents lists available at ScienceDirect

Journal of Arid Environments

journal homepage: www.elsevier.com/locate/jaridenv

Field validation of 1930s aerial photography: What are we missing?

D.M. Browning [a,*], S.R. Archer [a], A.T. Byrne [b]

[a] School of Natural Resources, University of Arizona, P.O. Box 210043, Tucson, AZ 85721, USA
[b] Department of Environmental Science & Policy and Biology, Clarkson University, 8 Clarkson Avenue, Potsdam, NY 13699, USA

ARTICLE INFO

Article history:
Received 14 August 2008
Received in revised form
5 March 2009
Accepted 3 April 2009
Available online 2 May 2009

Keywords:
Aboveground woody biomass
Detection limits
Error assessment
Historic aerial photography
Land cover
Panchromatic
Prosopis velutina
Retrospective ground truth
Retrospective mapping
Santa Rita experimental range
Sonoran Desert
Velvet mesquite

ABSTRACT

Aerial photography from the 1930s serves as the earliest synoptic depiction of vegetation cover. We generated a spatially explicit database of shrub (*Prosopis velutina*) stand structure within two 1.8 ha field plots established in 1932 to address two questions: (1) What are the detection limits of panchromatic 1936 aerial photography?, and (2) How do these influence *P. velutina* biomass estimates? Shrub polygons were manually digitized on 1936 imagery and linked to 1932 field measurements of *P. velutina* canopy area. Aboveground 1932 *P. velutina* biomass was estimated using a site-specific allometric relationship for field-measured canopy area. Shrub canopy detection limits on the 1936 imagery were comparable to those reported for contemporary imagery. Based on a conservative shrub size detection threshold of 3.8 m^2, 5.8% of *P. velutina* biomass was missed. Spatial resolution (0.6 vs. 1.0 m) did not influence detection limits, but the overall accuracy of shrub cover estimates was greater on 1.0 m images. Presence of the sub-shrub *Isocoma tenuisecta* may also have significantly influenced estimates of *P. velutina* canopy area. These analyses illustrate the importance of standardizing aerial photo interpretation protocols, accounting for uncertainty estimating shrub biomass, and caution species-specific interpretations for historic aerial photography.

Published by Elsevier Ltd.

1. Introduction

Changes in land cover and land use play a pivotal role in driving global change (Pielke et al., 2002; Vitousek, 1994). Historical perspectives enable researchers to elucidate trends and patterns of change and to disentangle interactions among factors influencing change trajectories (Foster et al., 2003). Aerial photography is useful for making quantitative multi-temporal assessments of land cover change. The synoptic nature and length of record provide the ability to map and monitor resources over large areas at decadal time scales. Commercial aerial photography in the United States was first available after World War I (Lillesand and Kiefer, 2000) and is the earliest source of remotely sensed imagery capturing land surface characteristics. As such, early aerial photography serves as the baseline for the longest time series of imagery and is broadly accessible through archival outlets [e.g., U.S. National Archives and Records Administration (NARA); Rango et al. (2008)].

A valuable component of the historic record, early aerial photography provides an important source of baseline assessments for studies of land cover change and an effective way to monitor long-lived plant species in a manner not generally possible in plot or experimental studies (Archer, 1996; Archer and Bowman, 2002; Fensham and Fairfax, 2002). The earliest aerial photography available in the southwestern United States was acquired in the mid-1930s as part of agricultural surveys conducted by the Agricultural Stabilization and Conservation Service and Soil Conservation Service (Rango et al., 2008). Because early aerial photos provide a basis from which to gauge the rate and extent of land cover and land use change, insights regarding detection limitations are relevant for land managers as well as members of the remote sensing, landscape ecology, forestry, and the ecosystem/global change modeling community. Land use and land cover change analyses based on remotely sensed imagery requires prudent evaluation of accuracy and performance (Rindfuss et al., 2004). However, there are no published records documenting the detection limits and accuracy of vegetation cover estimates derived from early aerial photography due to paucity of spatially explicit field data coincident with photo acquisition.

* Corresponding author at: USDA-ARS, Jornada Experimental Range, P.O. Box 30003, MSC 3JER, New Mexico State University, Las Cruces, NM 88003-8003, USA. Tel.: +1 575 646 2961; fax: +1 575 646 5889.
E-mail address: dbrownin@nmsu.edu (D.M. Browning).

0140-1963/$ – see front matter Published by Elsevier Ltd.
doi:10.1016/j.jaridenv.2009.04.003

One of the most striking land cover changes in grasslands and savannas (hereafter "rangelands") worldwide over the past 150 years has been the proliferation of trees and shrubs (hereafter "woody plants") at the expense of perennial grasses (Archer, 1995; Van Auken, 2000). Rangelands occupy ca. 40% of the global land surface (Bailey, 1996), contribute 30–35% of the terrestrial net primary productivity (Field et al., 1998), and are inhabited by more than two billion people (Safriel and Adeel, 2005). This land cover change in rangelands thus has ramifications for terrestrial carbon, nitrogen, and hydrologic cycles, land surface–atmosphere interactions, and rangeland and human health. Although regarded as having had a significant impact on the North American terrestrial carbon sink (Houghton, 2003; Pacala et al., 2001), the lack of detailed or spatially explicit historical records on this shift in land cover has hindered quantitative assessments.

An improvement in our ability to accurately estimate vegetation biomass across large areas is required to reduce uncertainty in terrestrial carbon pool estimates (Schimel et al., 2006). Time series analysis of repeat aerial photography or a combination of aerial photography and satellite imagery is one tool for addressing shortfalls in the historic land cover record (Asner et al., 2003). However, the utility of aerial photography for quantifying trends and patterns of woody plant cover in rangelands depends upon a variety of factors, including photo scale, atmospheric haze, spatial resolution or cell resolution size, and film development and digital image processing protocols (Fensham and Fairfax, 2002; Fensham et al., 2002). These factors can be assessed in modern photography (e.g., Fensham and Fairfax, 2007; Robinson et al., 2008). In contrast, historical photography, the baseline on which rates, patterns and trajectories of change are based, is not typically amenable for validation. Thus, we are forced to assume that detection limits in early images are comparable to those in more recent images. How robust is this assumption?

Cell resolution or photo grain size imposes constraints on the ability to distinguish landscape elements with remotely sensed imagery. Understanding these limitations is key to devising appropriate analytical methods to achieve study objectives (Woodcock and Strahler, 1987). The importance of spatial scale and the interactions between scale of measurement, discrete versus continuous depictions of landscape parameters, and spatial autocorrelation structure within an image has been recognized. Strahler et al. (1986) proposed a framework for exploring a range of natural resource applications with remote sensing models based upon the relationship between the size of analytical elements or image objects (e.g. shrub canopies) and cell resolution size. They used the term "H-resolution" to represent situations in which the targets of interest are larger than the cell resolution size (e.g., shrub canopies in fine spatial resolution aerial photography). Image objects are functionally defined by H-resolution pixel groups with similar appearance, tone, and structure (Hay et al., 1997). In H-resolution images, objects are discernable and spatial arrangement can be explored. Alternatively, the term "L-resolution" denotes situations in which target image objects are smaller than the cell resolution size (e.g., shrub canopies in moderate spatial resolution satellite imagery) and detection of individuals is not possible (Strahler et al., 1986). Both L- and H-resolution information exist in a given image (Woodcock and Strahler, 1987), thereby presenting a case for multiscale analytical approaches and clear definition of object-based research goals (Hay et al., 2003). Our analysis of 1936 panchromatic digitized imagery was based on the H-resolution model, wherein we specify one target, canopies of the dominant woody species (*Prosopis velutina* Woot.), to determine detection limitations of 1936 photography and validate aerial photo-based depictions of *P. velutina* canopies and landscape-scale estimates of shrub cover.

These objectives were addressed in Sonoran Desert grasslands of the southwestern U.S.A. where shrub encroachment has been well-documented (Brown, 1950; Browning et al., 2008; Glendening, 1952; McClaran, 2003). In 1932, two 40 m × 440 m plots were established on the Santa Rita Experimental Range in southeastern Arizona and the location of all shrubs and cacti within the plots were noted and their canopies measured (Glendening, 1952). This provided us with the unique opportunity to compare 1932 field maps of shrub canopy to cover maps derived from 1936 digital aerial photography. Specifically, we (1) validated estimates of shrub canopy cover at two scales of observation: *i*) individual *P. velutina* canopies and *ii*) total cover of all shrubs; (2) quantified the size of *P. velutina* plants below the detection limits on 1936 panchromatic imagery; (3) classified omission errors (*P. velutina* plants present in 1932 but not recognized on 1936 photography) attributable to *i*) detection limits, *ii*) spatial co-registration, and *iii*) species identification errors; and (4) translated detection limits to *P. velutina* biomass missed with the historic aerial photography. In addition, we (5) quantified the effect of image spatial resolution on detection limits and cover estimates by evaluating geometrically corrected digital imagery at two cell resolution sizes commonly used in studies of land cover change (0.6 and 1.0 m).

2. Methods

2.1. Study site

The study was conducted on the 21,514-ha Santa Rita Experimental Range (SRER) 45 km south of Tucson, Arizona (31° 49′ 58″ N, 110° 52′ 24″ W) along the western edge of the semi-desert grassland region of the Sonoran Desert as defined by Brown (1994). We focused on two 1.8 ha (40 m × 440 m) study plots at 1070 m elevation. Established in 1932 by Dr. William McGinnies in a mesquite savanna, the vegetation in these plots was representative of the semi-desert grasslands within the southwestern U.S.A. The McGinnies plots were situated on soils of late Pleistocene age with a sandy clay loam subsurface texture (Batchily et al., 2003). *P. velutina* (Woot.) was the dominant shrub. Other shrub species in the area included *Celtis pallida* Torr. and *Acacia gregii* Gray, and the sub-shrub *Isocoma tenuisecta* Greene, a species intermediate in growth form and longevity between herbaceous plants and true shrubs (Table 1). See McClaran et al. (2003) for detailed descriptions of geomorphology, vegetation, and climate.

Aerial photo validation was based on an exhaustive 1932 census of woody plant canopies within the two 1.8 ha plots situated ca. 60 m apart from each other (hereafter referred to as 'North' and 'South'). In the 1932 survey, corners of 10 m × 10 m subplots were marked with re-bar, and the location of all shrubs and cacti was mapped by species using a telescopic alidade and plane table and their canopy diameter recorded (Glendening, 1952). Sub-shrubs such as *I. tenuisecta* were not mapped. In 2006, we mapped subplot corners with a Global Positioning System (Leica GS20) using the Universal Transverse Mercator (UTM) projection, North American Datum 1983, while applying a 0.5 m horizontal positional accuracy threshold.

2.2. 1932 Field measurements

Shrubs locations in the 40 m × 440 m plots were incorporated into a geographic information system (GIS) by scanning and spatially registering 1932 scaled, hand-drawn survey maps to a Cartesian coordinate system in ArcMap (v.9.0 Environmental Science Research Institute Inc., 2004). Shrub locations on the geocoded 1932 field maps were digitized as points located at the bole of the largest stem. Because our objectives were to quantify the cover of true shrubs, cactus locations were not digitized. Field measurements of canopy diameter in North–South direction were

Table 1
Number and canopy area (mean, minimum and maximum; m^2) of woody plant species within two (North, South) 1.8 ha plots in 1932; data collected by Dr. William McGinnies (SRER Archives).

	North plot				South plot			
	No. of plants	Mean (SE)	Min	Max	No. of plants	Mean (SE)	Min	Max
Prosopis velutina	308	5.23 (0.49)	0.01	63.62	296	3.36 (0.32)	0.01	38.49
Acacia gregii	5	2.05 (0.76)	0.79	4.91	17	2.79 (0.76)	0.01	10.18
Celtis pallida	3	18.04 (9.83)	0.28	34.21	2	3.73 (3.34)	0.38	7.07
Mimosa aculeaticarpa var. *biuncifera*	0	–	–	–	1	–	0.13	0.13
Ephedra trifurca	0	–	–	–	4	0.65 (0.09)	0.38	0.79
Ziziphus obtusifolia	3	3.81 (1.99)	0.20	7.07	1	–	4.91	4.91

used to project shrub canopy area as that of a circle centered on the point location. Polygons representing woody plant canopies were then re-projected from Cartesian to UTM coordinate space (RMS Error = 0.270 m) in ArcMap for comparison with canopies digitized on the 1936 UTM-projected imagery.

To appraise validity of our assumption that *P. velutina* canopies were circular, we quantified an index of canopy asymmetry for 26 randomly selected *P. velutina* plants using circular statistical protocols outlined in Aradóttir et al. (1997). Field measurements of canopy radius (bole to the canopy edge) in eight (cardinal and intercardinal) directions were taken on each plant. We computed the mean vector of canopy dimensions, *r*, as an index denoting the degree of asymmetry. The vector length of *r* ranges from zero to unity, with the value of zero indicating a symmetrical distribution of canopy dimensions for which a mean angle of asymmetry is undefined (Zar, 1998). The mean *r* for the 26 plants measured was 0.02 (range = 0.01–0.15) and did not differ significantly from zero (Rayleigh's $Z = 0.01$).

2.3. Prosopis velutina *biomass*

Aboveground biomass (leaves + stems) of *P. velutina* plants measured in plots in 1932 was estimated using an existing site-specific canopy area allometric algorithm (see Browning et al., 2008). The proportion of *P. velutina* biomass potentially missed on photos across a range of detection thresholds was derived using the cumulative distribution of *P. velutina* plant mass across the range of canopy sizes.

2.4. 1936 aerial photography

Film negatives of panchromatic February 1936 aerial photographs (1:31,640) were acquired from NARA and scanned at 21 microns (1200 dpi) using an Epson Expression large format scanner. Vignetting effects, distortion along photo frame edges, were minimized by selecting the image with the McGinnies plots located near its center. This image was subset, geometrically corrected, and registered to the UTM projection by performing an image-to-image registration with 40 ground control points on an ortho-rectified digital ortho-quarter quadrangle (DOQQ) from the U.S. Geological Survey (Root Mean Square Error = 0.002 m). To evaluate the effect of spatial resolution on detection limits and estimates of woody plant cover, geo-coded 1936 images were generated at two cell resolutions corresponding to that of commercially available high-resolution satellite imagery commonly used to extract features of interest [i.e., Quickbird and IKONOS: 0.6 m and 1.0 m (Laliberte et al., 2004; Robinson et al., 2008)].

A protocol was established to standardize what constituted a shrub canopy (to be digitized) and the level of detail used to delineate shrub polygons. With a standardized protocol across a narrow range of spatial resolutions, we isolated the effects of cell resolution size on detection limits of the 1936 aerial photography. When resampling the digital imagery from 0.6 to 1.0 m resolution, a potential exists for the dominant image objects (i.e., large shrub canopies) to disproportionately influence the aggregated signal in the resampled image (Hay et al., 2001). However, in our case the range in cell resolution size was very small (0.6–1.0 m) and at the extreme low end of the *P. velutina* canopy size range (<1 m^2 to ca. 64 m^2), thereby dampening the role of upscaling error in our assessment of the effects of spatial resolution. To minimize observer bias, one author (AB) digitized all shrub polygons on the 0.6 and 1.0 m resolution images using feature editing tools in ArcMap. To maintain consistent detail in creating polygons, the digitizing process was performed in stream mode, which placed vertices every 2 m along the object perimeter. Pre-defined magnification levels that balanced magnification level and the ability to confidently discern canopies and their outlines were used. The radiometric resolution (8-bit) of the panchromatic image band along with photo scale rendered manual interpretation problematic at very high magnification levels as object boundaries were blurred. Discernable shrubs were initially identified by on-screen digitizing of canopies at 1:1250 or 1:800 magnifications. Once canopies were identified, their size and shape were refined on the basis of tonal and texture contrasts with surrounding pixels. Area and perimeter of manually digitized canopies were derived in ArcMap using Hawth Tools integrated with ESRI software (Beyer, 2004).

2.5. Image validation and error categorization

The shrub cover map digitized from the 1936 image was overlaid on the 1932 field map of shrub canopies to determine the extent to which the aerial photo estimates approximated field-based estimates (Fig. 1). In addition to identifying plants not accounted for on the 1936 image, we assessed two common types of error in photo interpretation: data co-registration and observer bias. Co-registration errors corresponded to the inability to confidently link digitized canopies on the photo to non-overlapping plant canopies (buffered 1 m) from field maps. We defined observer bias in the photo interpretation process as selective discrimination in what was defined as a plant canopy on the 1936 image. Cases of observer bias occurred amidst medium tones that lacked texture or discrete shape, such as might coincide with dense herbaceous cover. *P. velutina* plants mapped in the field in 1932 not corresponding to a canopy on the digitized aerial photo were categorized as "missed" due to: (1) spatial co-registration error, (2) observer bias when the tone, shape, and texture of the canopy was not sufficiently distinct to warrant classification as a 'shrub' image object, or (3) detection limits as there was no perceivable image object. In our comparison of field- vs. image-generated maps, small *P. velutina* plants beneath canopies of larger plants ($n = 14$ of 604) were excluded from the analysis of detection limitations, but were

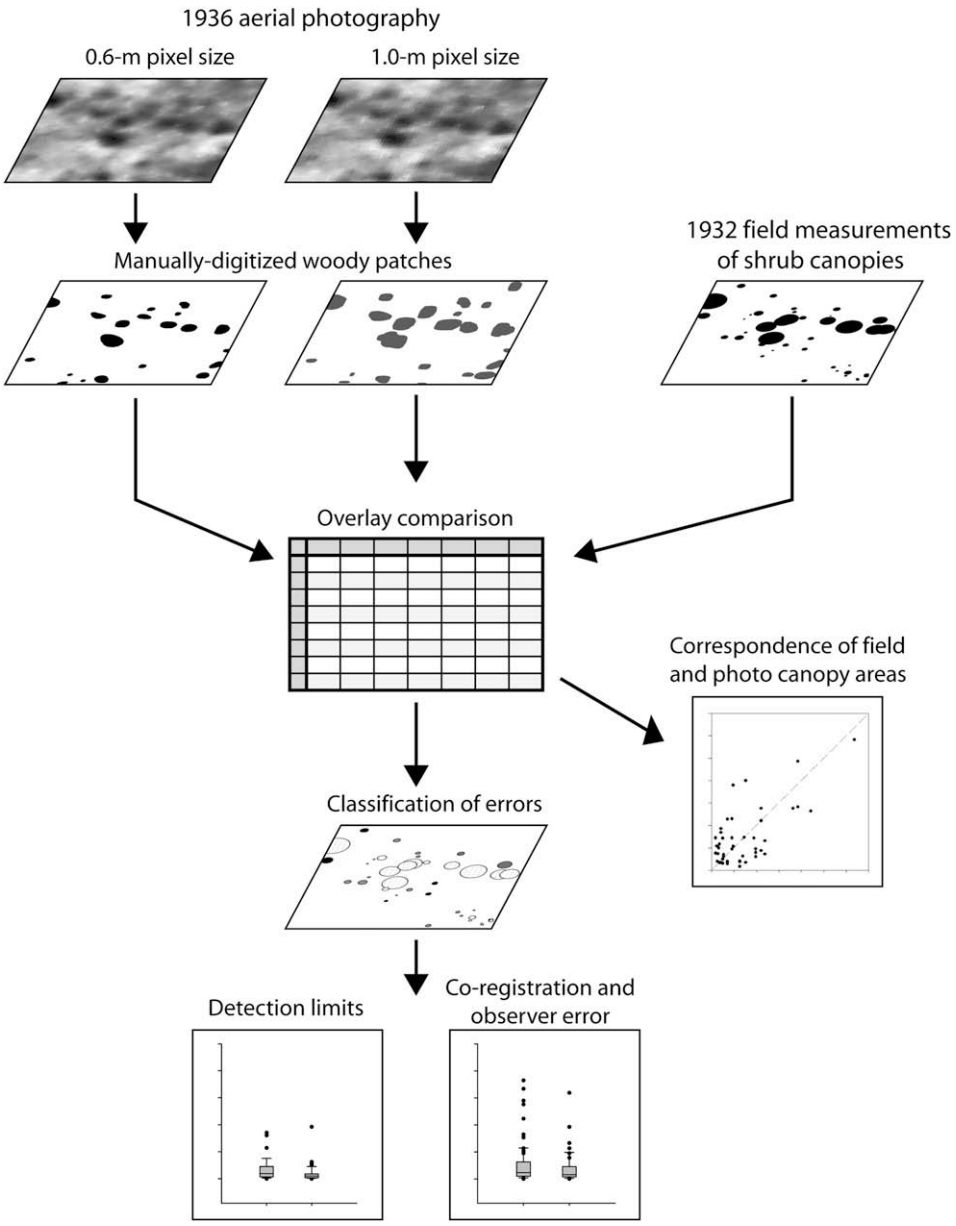

Fig. 1. Process flow diagram for validating shrub cover and *Prosopis velutina* biomass, and quantifying detection limits of 1936 panchromatic aerial photography using 1932 field maps of shrub canopies. Shrub species occurring in the plots are listed in Table 1.

included in estimates of *P. velutina* biomass missed with 1936 photography.

2.6. Validation of aerial photo woody cover estimates

To what extent can historical aerial photography be used to ascertain the canopy area of individual shrubs, and thus characterize the size-class distribution of plants on a site? How accurately does historic aerial photography depict woody plant cover at larger spatial extents? To address these questions, we validated photo estimates at two spatial scales: individual *P. velutina* canopies and total shrub cover across the 3.6 ha study area. We compared measurements of plant canopy area derived from 1936 photography at 0.6 and 1.0 m resolutions to field measurements of plant canopy area in 1932 graphically to characterize the relationship relative to the 1:1 line. Two-tailed *t*-tests were used to evaluate whether the slope of the line characterizing the correspondence between field and photo estimates was statistically different from 1.0. The canopy size validation exercise was limited to single *P. velutina* plants whose canopies on field maps were separated from the canopies of their neighbors by at least 1 m.

At the 3.6 ha extent of the study plots, spatial heterogeneity in vegetation cover, species composition, and plant density influence total cover estimates on aerial photos. To assess plot-scale estimates of total woody cover, we compared estimates from 1936 photos at 0.6 and 1.0 m spatial resolutions to that on 1932 field maps. In this plot-scale assessment, boundaries of overlapping shrub canopies on field maps were dissolved to represent woody plant cover from an aerial, top-down perspective. Portions of shrub canopy polygons on photos and field maps beyond plot boundaries were excluded, such that percent woody cover was computed as total shrub canopy area within plot (m^2) divided by plot size (m^2).

Species contributions to total woody plant cover were generated following the manual assignment of digitized 1936 shrub canopies

on 0.6 and 1.0 m imagery to species-specific field data. To standardize the species identification process, we applied a 1 m buffer to dissolved 1932 field polygons. When 1936 photo canopies overlapped 1932 field canopies within one meter and canopy size and position corresponded, it was manually assigned the species value. If a 1936 digitized canopy did not correspond (in location or size) to a mapped species of woody plant canopy, it was labeled "Other."

3. Results

3.1. Detection limits

P. velutina plants not discernable on the 1.0 m image were also not discernable on the 0.6 m image. Thus, resampling the 0.6 m resolution image to 1.0 m did not influence detection capabilities for individual plant canopies. Canopy area of undetected plants ranged from 0.01 to 9.6 m^2. Mean ($\pm$1 SE) canopy size of undetected *P. velutina* plants on the North plot (1.7 ± 0.3 m^2) was significantly greater than that of plants on the South plot (0.9 ± 0.2 m^2; $t = 2.37$, df = 46, $p = 0.021$) and variances associated with means were unequal (folded $F = 2.3$, df = 47, $p = 0.002$). Therefore, results were not pooled (Fig. 2A). Two additional sources of error are represented in Fig. 2B. Co-registration errors and observer bias accounted for the omission of a number of 1932 *P. velutina* canopies (up to 19.6 m^2 canopy area) on the 1936 photo overlay. These sources of error are inherent to studies involving manual interpretation of aerial photography and highlight the importance of gauging their influence on results from studies of land cover change. However, our emphasis remains on the detection limitations of early aerial photography.

To illustrate the influence of detection limitations on estimates of *P. velutina* aboveground biomass, we used a 3.8 m^2 canopy area detection threshold. This represents the 90th percentile for canopies not detected on 1936 images (inset, Fig. 2A) and limits the undue influence of the largest missing plants. Canopies ≤ 3.8 m^2 comprised 5.8% of *P. velutina* biomass ($n = 436$, Fig. 3). Spatial, spectral, and radiometric resolution clearly influence detection capabilities of remotely sensed imagery. Imagery with a cell resolution = 4 m (e.g., IKONOS) would have a minimum mapping unit of 16 m^2 and would miss approximately 30% of *P. velutina* biomass made up of ~654 individuals. The non-linear relationship between canopy size and aboveground biomass is illustrated by the fact that >30% of *P. velutina* biomass in the plots was contributed by the 11 largest trees.

3.2. Validation of aerial photo woody cover estimates

The canopy area of *P. velutina* plants >20 m^2 in size was consistently under-estimated at the 0.6 m resolution with the slope of the line through the points deviating significantly from 1.0 ($t = -15.2$, df = 1, $p = 0.04$) (Fig. 4A). Canopies on the 1.0 m image were both under-and over-estimated relative to 1932 field measurements (Fig. 4B), with the slope of the regression line not differing from 1.0 ($t = -3.20$, df = 1, $p = 0.193$). Given that the 1932 field canopy measurement values in Fig. 4 are fixed (x-axis) at both cell resolution sizes, these differences in photo-derived estimates of *P. velutina* canopy area reflect the influence of spatial resolution on manual image interpretation.

Total shrub cover differed on the North and South plots, as did the contribution of less common species; yet, *P. velutina* clearly dominated woody plant cover (Fig. 5, Table 1). At the landscape scale, total shrub cover was under-estimated on the 0.6 m image by 37% (North plot) and 38% (South plot). At the 1.0 m resolution, shrub cover was over-estimated by 5% on the North plot and under-estimated by 13% on the South plot where mean *P. velutina* canopy size was statistically smaller (Fig. 2A). Contributions of *C. pallida* (North plot) and *A. gregii* (South plot) were accurately depicted at both spatial resolutions. Relative contributions of unidentified species to absolute shrub cover, consistent for 0.6 and 1.0 m images, ranged from 26% to 33% of total cover (Fig. 5).

Species composition of the ~70 polygons classified as 'Other' on the 1936 photography (Table 2) was possibly: (1) cacti (*Opuntia fulgida*, *Opuntia spinosior*, *Opuntia engelmannii*, *Echinocactus wislizeni*), (2) large patches of dense herbaceous ground cover, or (3) the sub-shrub, *I. tenuisecta*. The composition of the unknown patches

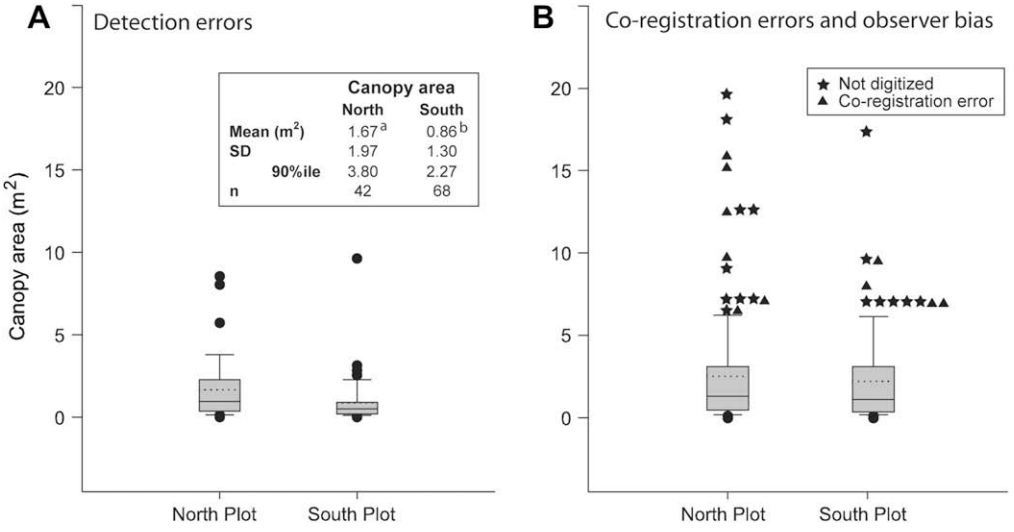

Fig. 2. Box and whisker plots of 1932 of *P. velutina* canopies missed on panchromatic (1:31,640) aerial photography acquired February 1936. Mean canopy area is illustrated with dotted horizontal lines, while canopies beyond the 90th percentile are represented with symbols. The inset table in Panel A summarizes descriptive statistics for *P. velutina* canopies on 1932 field maps that were not discernable on the photography. Panel B depicts 1932 *P. velutina* canopies missed on the 1936 image due to spatial co-registration and observer bias in the interpretation and delineation of image objects (i.e., shrub canopies). Canopies not perceived as discrete image objects (stars ★) or that did not overlap with digitized shrub canopies (triangles ▲) are shown. The same plants were missed at 0.6 and 1.0 pixel resolutions.

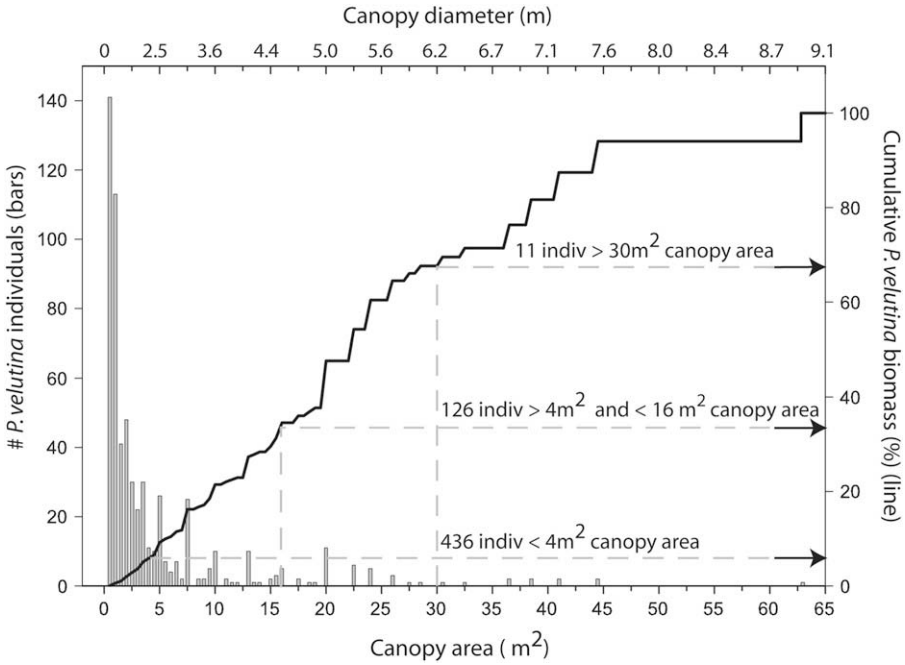

Fig. 3. Canopy size distribution (0.5 m^2 intervals; bars) and cumulative *P. velutina* aboveground biomass (line) based on 1932 field measurements in southeastern Arizona. Biomass was derived using an allometric equation (Browning et al., 2008). Dashed lines denote the number of plants and the proportion of *P. velutina* biomass that would be missed at canopy area detection thresholds of 4, 16, and 30 m^2. The two lowest thresholds correspond to detection limits of 1936 aerial photography (see Fig. 2A) and the cell resolution size for multispectral image bands from IKONOS, a commonly used source of high-resolution satellite imagery, respectively.

was likely not cacti because: (1) a visual inspection of cacti locations on geo-coded field maps indicated cactus did not spatially coincide with 'Other' image patches and (2) cactus density in 1932 was extremely low at 30 plants ha^{-1} and plants were not highly aggregated (Glendening, 1952). Composition of 'Other' was likely not herbaceous vegetation as average ground cover was only 0.8% on the mapped study plots (Glendening, 1952). However, the composition of 'Other' may have been *I. tenuisecta*. Canopies of this sub-shrub can approach detection limits [Fig. 6, SRER Archives (McClaran et al., 2002)] and multi-plant patches of this sub-shrub might be readily detected.

4. Discussion

Field data permitting validation of land cover estimates as far back as the 1930s are rare. We were interested in using early aerial photography as a baseline from which to reconstruct the rate and magnitude of changes in shrub cover and biomass in areas that were historically grasslands. By incorporating 1932 field maps of shrub canopies at the SRER generated by William McGinnies into a spatially explicit database, we were able to take advantage of a unique opportunity to critically evaluate the accuracy and limitations of 1936 aerial photos for this purpose.

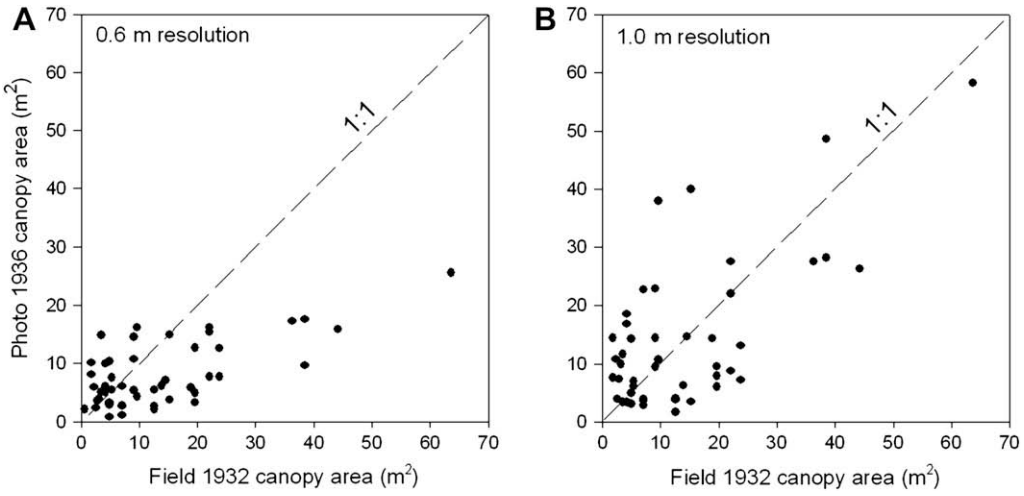

Fig. 4. Relationships between shrub canopy area manually digitized from panchromatic 1936 aerial photography (y-axis) and 1932 field-measured *Prosopis velutina* canopy area (x-axis) at two spatial resolutions: 0.6 m (A) and 1.0 m (B). Field measurements (x-axis) are the same in both panels; hence differences in 1936 photo-derived canopy area reflect those resulting from effects of spatial resolution. Only canopies corresponding to a single *P. velutina* plant were used in this analysis; multiple-plant patches were excluded.

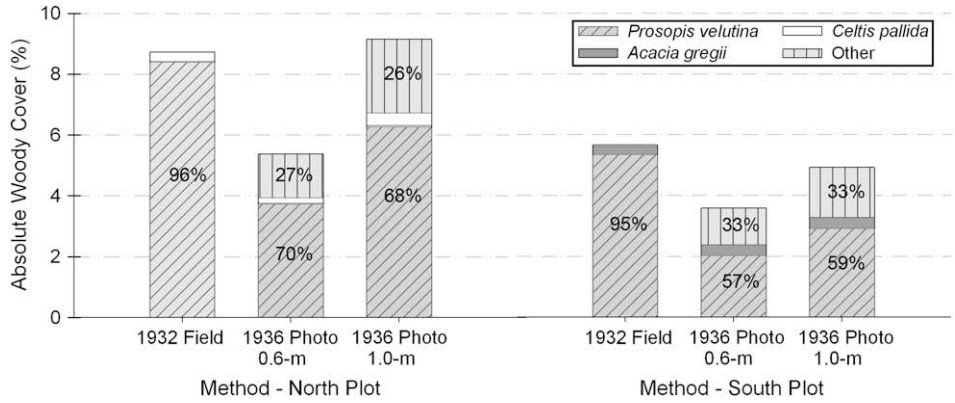

Fig. 5. Species-specific contributions to woody plant cover on the Santa Rita Experimental Range in southeastern Arizona based on 1932 field measurements (Table 1) and 1936 aerial photography manually digitized at 0.6 m and 1.0 m spatial resolutions for two 1.8 ha plots (North and South). Species assignments on the 1936 photograph were made by overlaying species-specific 1932 field maps of shrub cover. Polygons digitized as 'Shrubs' but that did not correspond to woody plants on the 1932 field maps (buffered by 1 m) were categorized as "Other." Relative (%) species contributions to absolute cover are indicated within each bar. Contributions of *Ephedra trifurca* and *Ziziphus obtusifolia* to total cover (not shown) were 0.01% and 0.03%, respectively.

4.1. Detection limits of 1930s aerial photography

The minimum mapping unit in remote sensing studies is commonly defined by the cell resolution (i.e., grain) size of imagery (e.g., Goslee et al., 2003). Our analyses suggest this assumption is too simplistic for 1936 panchromatic aerial photography where detection limits for our targets of interest (i.e., shrub canopies) were nearly four times the grain size. We found a substantial range of sizes of 'undetected' shrub canopies, but using a 90th percentile cutoff generated a minimum canopy area detection size of 3.8 m^2. This result compares favorably with detection limits ranging of 2.9–3.3 m^2 canopy area reported for woody plants in 1994 natural color digital imagery (1.4 m resolution) in Western Australia (Robinson et al., 2008). Thus, from a minimum detection limit standpoint, detection capabilities of the 1936 imagery were comparable with those obtained from modern imagery.

In our manual classification of 1936 imagery, we failed to discern three large *P. velutina* plants whose canopies were indistinguishable from the background matrix consisting of herbaceous and sub-shrub cover and bare soil components. Close inspection of field data and the spatial context of these individual *P. velutina* plants did not reveal an obvious reason for their misrepresentation. Although the three plants constituted <0.1% of total shrub canopy area and 0.6% of total *P. velutina* cover, they serve to highlight the importance of evaluating the distribution of canopy sizes not represented rather than simply choosing the maximum value to define the minimum mapping unit.

Table 2
Descriptive statistics for image objects manually digitized on 1936 aerial photography at two spatial resolutions (i.e., ground resolved distance) that did not correspond to the shrub species noted on 1932 field maps (see Table 1). In our species identification scheme, these patches were >1 m from the canopy edge of mapped species and classified as "Other."

Patch size (m^2)	Spatial resolution			
	0.6 m		1.0 m	
	North	South	North	South
n	40	32	39	30
Mean	5.9	6.6	10.6	9.1
SD	4.2	4.4	6.8	4.7
Min–Max	0.9–20.1	1.5–20.2	1.6–31.5	3.5–23.6

4.2. Field validation of woody plant cover

Our validation of shrub cover estimates from 1936 panchromatic aerial photography conducted at two spatial extents revealed biases at the level of individual canopies; yet in spite of these biases, total plant cover at the plot-scale was accurately delineated. Results indicate caution must be exercised when using historic aerial photography for species-specific cover or biomass assessments. Effects of shadow on photo-derived estimates of canopy area and shrub cover occur at both individual canopy and landscape scales. Metadata needed to correct for shadow and atmospheric conditions were unavailable, as is commonly the case with archive aerial photography (Rango et al., 2008). However, the correspondence between field-measured and 1.0 m photo image canopy areas suggests shadow on the 1936 image may not have been significant. Flat terrain (<3% slope) and the February acquisition date (when the deciduous shrubs would have been largely leafless in this subtropical system) likely helped downplay the effects of shadow. Furthermore, shadow effects typically result in

Fig. 6. Dr. Robert R. Humphrey with a burroweed plant (*Isocoma tenuisecta*) 21 February 1935 [photo by Gibbs, Santa Rita Experimental Range Archive (No. 328920)]. Photo was taken adjacent to South McGinnies plot. Assuming a 2 m arm span, this subshrub would have a canopy area of ca. 3.1 m^2 in size, approaching the detection limits of the 1936 aerial photography. Widely scattered *Prosopis velutina* trees appear in the background within a grassy matrix.

overestimation of crown area (Fensham et al., 2002), not under-estimation as in our case. It appears that tone and texture distinctions between shrub canopies and background vegetation and soils were blurred at the 0.6 m resolution in a manner that caused shrub canopy area to be under-estimated.

4.2.1. Plant canopy-scale comparisons

Relative to the 0.6 m image, the 1.0 m spatial resolution yielded better estimates of area at the level of individual canopies. This result is counterintuitive to the expectation of enhanced image detail with finer spatial resolution; however, it corroborates results from Fensham and Fairfax (2007) who also observed that shrub canopies appear larger as photo scale decreases (i.e., coarsens). The correspondence between field-measured and photo-estimated canopy area for individual plants more closely approximated a 1:1 relationship with 1.0 m imagery. For the 1:31,640 imagery used in this study, the 1.0 m resolution appeared to provide optimal results for depicting *P. velutina* canopies.

We identified three sources of error that could potentially affect our results regarding detection limits and classification accuracy assessments. First, despite fastidious data handling and translation of the 1932 field data, spatial discrepancies due either to the field mapping process or to the digitizing of field maps may have occurred. This would have contributed to the co-registration errors in Fig. 2B. Measurement or transcription errors with canopy size would be of greater importance. We assume that errors would be random, with no reason to suspect otherwise. Second, aerial photo estimates of the canopy area of individual *P. velutina* plants may have been biased by the presence of *I. tenuisecta*. If we were unknowingly detecting large patches of this sub-shrub on the aerial photography (Fig. 6) and if the area of some *I. tenuisecta* patches adjacent to *P. velutina* plants were included in the photo measurements of *P. velutina* canopies, then over-estimates of *P. velutina* canopy area would result. Third, discrepancies between photo- and field-maps of shrub cover can occur if photo acquisition and field measurement dates differ and are not accounted for (Fensham and Fairfax, 2002). Based on estimates of canopy expansion rates at this site [0.25 $m^2 y^{-1}$, Browning et al., 2008], the four years between field data collection and image acquisition could have resulted in an approximate 1.0 m^2 increase in *P. velutina* canopy area. Canopy growth between 1932 and 1936 would result in over-estimates of canopy size in the photography. We could not evoke potential canopy growth over four years to explain variability in canopy size estimates, as photo-measured *P. velutina* canopy size was not consistently over-estimated. Furthermore, this small adjustment would have minimal effect on the overall spread of points in Fig. 4, particularly for the larger (canopy area >20 m^2 area) plants.

4.2.2. Landscape-scale comparisons of cover

Factors in addition to those at the plant canopy-scale influenced the effects of spatial resolution on accuracy of shrub cover estimates across the 3.6 ha study area; namely *P. velutina* stand size structure and 1932 field mapping protocols. The degree to which *P. velutina* cover was under-estimated is partially a function of the abundance of plants below detection limits and their contribution to total shrub cover. While mean *P. velutina* canopy size in the South plot was smaller and there were more plants with canopies below 3.8 m^2 in size (237 versus 213 on the North plot), these plants made the same contribution to total shrub cover (1.4%) on both plots. The close correspondence between field and photo estimates of total shrub cover at 1.0 m appears to reflect the fact that underestimates of *P. velutina* cover, due in part to detection limitations, were compensated for by the contribution of 'Other' vegetation patches on the photo that were not mapped in the 1932 field census.

Unidentified vegetation patches that compensated for under-estimates of *P. velutina* cover represent a challenge for retrospective interpretation of historic aerial photography. Historical records and ground photographs suggest *I. tenuisecta*, intermediate in growth form and longevity between herbaceous plants and true shrubs, was the most likely species to contribute to the 'Other' vegetation patches (Fig. 6). This sub-shrub exhibits strong cyclic patterns of population growth and decline (McClaran, 2003). In 1934, the 5 km^2 area encompassing the McGinnies plots was classified as "heavily infested" with *I. tenuisecta* with over 3707 plants ha^{-1} (Humphrey and Mehrhoff, 1958; Mehrhoff, 1955). It seems reasonable to expect that conglomerate patches of this plant may have been evident on the 1936 image. Had the cover of *I. tenuisecta* been accounted for in the 1932 field map, field-measured shrub cover would have been higher and 1936 photo estimates of total woody cover would have been under-estimated to a somewhat greater extent than shown in Fig. 5. The presence of plants such as *I. tenuisecta* may complicate species-specific interpretation of cover and biomass estimates from aerial photography. As such, this retrospective field validation highlights an omnipresent challenge linking field data to remotely sensed estimates of cover.

4.3. Ramifications for biomass estimation

Remote sensing applications using time series aerial photography can be used for long-term retrospective and contemporary assessments of shrub biomass, but with several caveats. First, most remotely sensed imagery is not capable of discerning small members of the plant community, thereby missing the most dynamic portion of the population and compromising the ability to quantify woody plant size-class distributions. Recent advances with very high spatial resolution imagery from unmanned aerial vehicles (UAVs) are a notable exception (Rango et al., 2006). Although plants below detection thresholds (canopies <3.8 m^2 in our case) constituted only a small fraction of the total shrub biomass (ca. 6% in our case), a failure to account for them compromises our ability to forecast ecosystem productivity and carbon sequestration potential since carbon uptake is maximal in young stands and plateaus in mature stands (Hurtt et al., 2002). Remote sensing methods devised for L-resolution imagery (i.e., moderate spatial resolution) such as spectral mixture analysis, can quantify sub-pixel contributions of shrub cover, integrating the spectral response of all shrub constituents (regardless of size). Spectral mixture analysis is a viable alternative for effectively estimating woody biomass with multispectral imagery (Asner et al., 2003; Huang et al., 2007). However, such techniques do not generate object-based depictions for size-class determination and are not suitable for coarse spectral resolution imagery.

Second, assumptions regarding species or functional group composition should be clearly stated and, to the extent possible, evaluated. Species identification is not easily achieved remotely; and our case was no exception. Our original intent was to use estimates of aboveground biomass derived from shrub canopy cover on 1932 imagery as a basis from which to quantify rates and patterns of change using aerial photos in subsequent decades. Because *P. velutina* clearly dominated cover on the study site we assumed we could apply a canopy area-biomass algorithm developed for this species across the site. Although this algorithm would not necessarily be appropriate for other species on the site, 1932 field maps and contemporary field surveys indicated their abundances were low enough that errors would be minimal. However, as it turned out, 26–33% of the classified shrub cover on the 1936 image was attributable to 'Other' species, potentially *I. tenuisecta*, not recorded in field maps. A 5 m^2 canopy (2.5 m canopy diameter) *P. velutina* plant would have 7.3 kg dry weight aboveground

biomass (allometric relationship from Browning et al., 2008), whereas an *I. tenuisecta* sub-shrub of comparable canopy area would have a mass of 6.1 kg (allometric relationship from Huang et al., 2007). Thus, if *I. tenuisecta* comprised the 'Other' fraction of total shrub cover and the *P. velutina* algorithm was applied, aboveground woody biomass would be over-estimated by ca. 20%. In the absence of metadata, there is little recourse in correcting these errors on historic aerial photography. Yet, these data suggest modern biomass estimates could be improved with directed field surveys and the integration of available historic data to determine species composition (Andersen, 2006).

Finally, the inability to discern individual plant canopies in satellite or airborne imagery is a function of the spatial, spectral, and radiometric resolution of the sensor, shadow, canopy architecture, and plant density. In cases where canopies of individuals of the same or differing species meet or overlap, it cannot be reliably determined from a top-down perspective whether a given image object represents one large plant, multiple plants of the same species, or multiple plants of differing species. We circumvented this problem by focusing our analyses of canopies digitized on the aerial photos known to correspond to single *P. velutina* plants mapped in 1932 and limiting application of the species-specific allometric algorithm to field measurements of individual *P. velutina* canopies. For many woody plants, including *Prosopis*, biomass increases exponentially with canopy area (Northup et al., 2005). Thus, representing an entity as a single large plant, when it is in fact a group of smaller plants could substantially over-estimate biomass. This problem is not unique to the 1930s photography; and it also presents challenges for more recent aerial photography (Browning et al., 2008). Resolving this problem may not be possible on historical photos, but contemporary estimates of biomass from high-resolution remotely sensed imagery could be potentially improved by incorporating field surveys, LIDAR-based estimates of shrub height and patch structure (Vega and St-Onge, 2008) or very high-resolution imagery from UAVs (Rango et al., 2006).

5. Summary

Rangelands undergoing shifts from grass- to woody plant-domination across broad spatial extents represent can profoundly alter aboveground biomass (Knapp et al., 2008) and challenge efforts aimed at quantifying and monitoring ecosystem primary production and carbon stocks (Houghton et al., 1999). Repeat aerial photography is a valuable tool for reconstructing change in woody plant cover and biomass in rangelands over decadal time scales, and over areas much larger than those possible from ground-based surveys. Aerial photos from the 1930s can be used to establish baseline conditions from which to assess rates and patterns of subsequent change. Taking advantage of a historic spatially explicit field data set from 1932, we were able to explore the detection limitations and accuracy of woody cover and biomass estimates from 1936 aerial photography. Spatial resolution did not influence detection limits, but the overall accuracy of shrub cover estimates was greater on 1.0 m than on 0.6 m resolution images. Information extracted from historic 1936 aerial photo images was on par with what can been extracted from more recent aerial photography and enables informed, long-term, and spatially explicit assessments of woody cover change in rangelands.

Acknowledgments

The historic legacy of W. McGinnies is recognized and extraordinary. R. Wu assisted with data compilation and fastidious quality assurance. A. Honaman graciously provided technical assistance with computing logistics with resources provided by the University of Arizona, School of Natural Resources. The historic ground photograph and field maps were provided by the Santa Rita Experimental Range Digital Database (http://ag.arizona.edu/srer). S. Marsh and A. Huete made helpful comments on early drafts. A. Aradóttir provided advice on circular statistics. A. Rango, M. Buenemann, and two anonymous reviewers provided additional editorial suggestions that improved the manuscript. D. Browning was supported by a United States Environmental Protection Agency (EPA) Science to Achieve Results Graduate Fellowship FP-91637801-3; A. Byrne was supported by the NSF Research Experience for Undergraduate Program. Additional funding was provided by NASA Grant NAG5-11238, NSF DEB-9981723, and a T&E, Inc. Conservation Biology Grant. EPA has not officially endorsed this publication and the views expressed herein may not reflect the views of the EPA.

References

Andersen, G.L., 2006. How to detect desert trees using CORONA images: discovering historical ecological data. Journal of Arid Environments 65, 491–511.
Aradóttir, A.L., Robertson, A., Moore, E., 1997. Circular statistical analysis of birch colonization and the directional growth response of birch and black cottonwood in south Iceland. Agricultural and Forest Meteorology 84, 179–186.
Archer, S., 1995. Tree–grass dynamics in a *Prosopis*-thornscrub savanna parkland: reconstructing the past and predicting the future. Ecoscience 2, 83–99.
Archer, S., 1996. Assessing and interpreting grass-woody plant dynamics. In: Hodgson, J., Illius, A. (Eds.), The Ecology and Management of Grazing Systems. CAB International, Wallingford, Oxon, United Kingdom, pp. 101–134.
Archer, S., Bowman, A., 2002. Understanding and managing rangeland plant communities. In: Grice, A.C., Hodgkinson, K.C. (Eds.), Global Rangelands: Progress and Prospects. CAB International, Wallingford, Oxon, United Kingdom, pp. 63–80.
Asner, G.P., Archer, S., Hughes, R.F., Ansley, R.J., Wessman, C.A., 2003. Net changes in regional woody vegetation cover and carbon storage in Texas drylands, 1937–1999. Global Change Biology 9, 1–20.
Bailey, R.G., 1996. Ecosystem Geography. Springer, New York, NY, USA.
Batchily, A.K., Post, D.F., Bryant, R.B., Breckenfeld, D.J., 2003. Spectral reflectance and soil morphology characteristics of Santa Rita experimental range soils. In: McClaran, M.P., Ffolliott, P.F., Edminster, C.B. (Eds.), Santa Rita Experimental Range: One-Hundred Years (1903–2003) of Accomplishments and Contributions. Conference Proceedings, 30 October–1 November 2003, Tucson, AZ.U.S. Department of Agriculture, Forest Service, Rocky Mountain Research Station, Ogden, UT, pp. 175–182.
Beyer, H.L., 2004. Hawth's Analysis Tools for ArcGIS. Available at http://www.spatialecology.com/htools.
Brown, A.L., 1950. Shrub invasion of a southern Arizona desert grassland. Journal of Range Management 3, 172–177.
Brown, D.E., 1994. Semidesert grassland. In: Brown, D.E. (Ed.), Biotic Communities: Southwestern United States and Northwestern Mexico. University of Utah Press, Salt Lake City, UT, USA, pp. 123–131.
Browning, D.M., Archer, S.R., Asner, G.P., McClaran, M.P., Wessman, C.A., 2008. Woody plants in grasslands: post-encroachment dynamics. Ecological Applications 18, 928–944.
Environmental Science Research Institute Inc., 2004. ArcGIS, v. 9.0. Redlands, CA, USA.
Fensham, R.J., Fairfax, R.J., 2002. Aerial photography for assessing vegetation change: a review of applications and the relevance of findings for Australian vegetation history. Australian Journal of Botany 50, 415–429.
Fensham, R.J., Fairfax, R.J., 2007. Effect of photoscale, interpreter bias and land type on woody crown-cover estimates from aerial photography. Australian Journal of Botany 55, 457–463.
Fensham, R.J., Fairfax, R.J., Holman, J.E., Whitehead, P.J., 2002. Quantitative assessment of vegetation structural attributes from aerial photography. International Journal of Remote Sensing 23, 2293–2317.
Field, C.B., Behrenfeld, M., Randerson, J., Falkowski, P., 1998. Primary production of the biosphere: integrating terrestrial and oceanic components. Science 281, 237–240.
Foster, D., Swanson, F., Aber, J., Burke, I., Brokaw, N., Tilman, D., Knapp, A., 2003. The importance of land-use legacies to ecology and conservation. Bioscience 53, 77–88.
Glendening, G.E., 1952. Some quantitative data on the increase of mesquite and cactus on a desert grassland range in southern Arizona. Ecology 33, 319–328.
Goslee, S., Havstad, K.M., Peters, D.P.C., Rango, A., Schlesinger, W.H., 2003. High-resolution images reveal rate and pattern of shrub encroachment over six decades in New Mexico, USA. Journal of Arid Environments 54, 755–767.
Hay, G.J., Blaschke, T., Marceau, D.J., Bouchard, A., 2003. A comparison of three image-object methods for the multiscale analysis of landscape structure. ISPRS Journal of Photogrammetry and Remote Sensing 57, 327–345.

Hay, G.J., Marceau, D.J., Dube, P., Bouchard, A., 2001. A multiscale framework for landscape analysis: object-specific analysis and upscaling. Landscape Ecology 16, 471–490.

Hay, G.J., Niemann, K.O., Goodenough, D.G., 1997. Spatial thresholds, image-objects, and upscaling: a multiscale evaluation. Remote Sensing of Environment 62, 1–19.

Houghton, R.A., 2003. Revised estimates of the annual net flux of carbon to the atmosphere from changes in land use and land management 1850–2000. Tellus 55B, 378–390.

Houghton, R.A., Hackler, J.L., Lawrence, K.T., 1999. The U.S. carbon budget: contributions from land-use change. Science 285, 574–578.

Huang, C.Y., Marsh, S.E., McClaran, M.P., Archer, S.R., 2007. Postfire stand structure in a semiarid savanna: cross-scale challenges estimating biomass. Ecological Applications 17, 1899–1910.

Humphrey, R.R., Mehrhoff, L.A., 1958. Vegetation changes on a southern Arizona grassland range. Ecology 39, 720–726.

Hurtt, G.C., Pacala, S.W., Moorcroft, P.R., 2002. Projecting the future of the U.S. carbon sink. Proceedings of the National Academy of Sciences 99, 1389–1394.

Knapp, A.K., Briggs, J.M., Collins, S.L., Archer, S.R., Bret-Harte, M.S., Ewers, B.E., Peters, D.P., Young, D.R., Shaver, G.R., Pendall, E., Cleary, M.B., 2008. Shrub encroachment in North American grasslands: shifts in growth form dominance rapidly alters control of ecosystem carbon inputs. Global Change Biology 14, 615–623.

Laliberte, A.S., Rango, A., Havstad, K.M., Paris, J.F., Beck, R.F., McNeely, R., Gonzalez, A.L., 2004. Object-oriented image analysis for mapping shrub encroachment from 1937 to 2003 in southern New Mexico. Remote Sensing of Environment 93, 198–210.

Lillesand, T.M., Kiefer, R.W., 2000. Remote Sensing and Image Interpretation, fourth ed. John Wiley & Sons, Inc., New York, NY, USA.

McClaran, M.P., Angell, D.L., Wissler, C., 2002. Santa Rita Experimental Range Digital Database: User's Guide. General Technical Report RMRS-GTR-100. USFS Forest Service Rocky Mountain Research Station, Ogden, UT, USA.

McClaran, M.P., 2003. A century of vegetation change on the Santa Rita experimental range. In: McClaran, M.P., Ffolliott, P.F., Edminster, C.B. (Eds.), Santa Rita Experimental Range: One-Hundred Years (1903–2003) of Accomplishments and Contributions. Conference Proceedings, 30 October–1 November 2003, Tucson, AZ, U.S. Department of Agriculture, Forest Service, Rocky Mountain Research Station, Ogden, Utah, pp. 16–33.

McClaran, M.P., Ffolliott, P.F., and Edminster, C.B. Technical Coordinators, 2003. Santa Rita Experimental Range: One-Hundred Years (1903–2003) of Accomplishments and Contributions. Conference Proceedings, 30 October–1 November 2003, Tucson, AZ, U.S. Department of Agriculture, Forest Service, Rocky Mountain Research Station, Ogden, UT.

Mehrhoff, L.A., 1955. Vegetation Changes on a Southern Arizona Grassland Range – An Analysis of Causes. M.S. University of Arizona, Tucson.

Northup, B.K., Zitzer, S.F., Archer, S.R., McMurtry, C.R., Boutton, T.W., 2005. Above-ground biomass and carbon and nitrogen content of woody species in a subtropical thornscrub parkland. Journal of Arid Environments 62, 23–43.

Pacala, S.W., Hurtt, G.C., Baker, D., Peylin, P., Houghton, R.A., Birdsey, R.A., Heath, L., Sundquist, E.T., Stallard, R.F., Ciais, P., Moorcroft, P., Caspersen, J.P., Shevliakova, E., Moore, B., Kohlmaier, G., Holland, E., Gloor, M., Harmon, M.E., Fan, S.M., Sarmiento, J.L., Goodale, C.L., Schimel, D., Field, C.B., 2001. Consistent land- and atmosphere-based U.S. carbon sink estimates. Science 292, 2316–2320.

Pielke, R.A., Marland, G., Betts, R.A., Chase, T.N., Eastman, J.L., Niles, J.O., Niyogi, D.D.S., Running, S.W., 2002. The influence of land-use change and landscape dynamics on the climate system: relevance to climate-change policy beyond the radiative effect of greenhouse gases. Philosophical Transactions of Royal Society of London 360, 1705–1719.

Rango, A., Laliberte, A., Steele, C., Herrick, J.E., Bestelmeyer, B., Schmugge, T., Roanhorse, A., Jenkins, V., 2006. Using unmanned aerial vehicles for rangelands: current applications and future potentials. Environmental Practice 8, 159–168.

Rango, A., Laliberte, A., Winters, C., 2008. Role of aerial photos in compiling a long-term remote sensing data set. Journal of Applied Remote Sensing 2, 1–21.

Rindfuss, R.R., Walsh, S.J., Turner, B.L., Fox, J., Mishra, V., 2004. Developing a science of land change: challenges and methodological issues. Proceedings of the National Academy of Sciences of the United States of America 101, 13976–13981.

Robinson, T.P., van Klinken, R.D., Metternicht, G., 2008. Spatial and temporal rates and patterns of mesquite (*Prosopis* species) invasion in Western Australia. Journal of Arid Environments 72, 175–188.

Safriel, U., Adeel, Z., 2005. Dryland systems. In: Hassan, R., Scholes, R., Ash, N. (Eds.), Ecosystems and Human Well-Being: Current State and Trends. Island Press, Washington, D.C., USA, pp. 623–662.

Schimel, D., Fung, I., Defries, R., 2006. Space-based ecological observations: the NASA decadal survey. Frontiers in Ecology and the Environment 4, 171.

Strahler, A.H., Woodcock, C.E., Smith, J.A., 1986. On the nature of models in remote-sensing. Remote Sensing of Environment 20, 121–139.

Van Auken, O.W., 2000. Shrub invasions of North American semiarid grasslands. Annual Review Ecology and Systematics 31, 197–215.

Vega, C., St-Onge, B., 2008. Height growth reconstruction of a boreal forest canopy over a period of 58 years using a combination of photogrammetric and lidar models. Remote Sensing of Environment 112, 1784–1794.

Vitousek, P.M., 1994. Beyond global warming: ecology and global change. Ecology 75, 1861–1876.

Woodcock, C.E., Strahler, A.H., 1987. The factor of scale in remote sensing. Remote Sensing of Environment 21, 311–332.

Zar, J.H., 1998. Biostatistical Analysis, fourth ed. Prentice Hall, Upper Saddle River, New Jersey.